PARAMETER ESTIMATION OF LFM SIGNAL INTERCEPTED BY SYNCHRONOUS NYQUIST FOLDING RECEIVER

D. Zeng[*], H. Cheng, J. Zhu, and B. Tang

School of Electronic Engineering, University of Electronic Science and Technology of China, Chengdu 611731, China

Abstract—Nyquist folding receiver (NYFR) is a new kind of interception architecture, which can simultaneously intercept wideband signals in multi-Nyquist zones with one or two analog-to-digital converters (ADCs). A parameter estimation algorithm of the linear frequency modulated (LFM) signal intercepted by an improved NYFR is presented. Firstly, the NYFR is improved by introducing a synchronous mechanism, and we denote this structure as a synchronous NYFR (SNYFR). Secondly, taking LFM as an example, the input and output noise distributions of an SNYFR are discussed. Then, a fast parameter estimation algorithm is derived from the frequency spectrum of the output signal, and an advice for the design of local oscillator signal is given. Simulations show that the parameter estimation accuracy is close to the maximum likelihood when the signal to noise ratio (SNR) is above -3 dB.

1. INTRODUCTION

Many modern radars have very high carrier frequencies or wide operating bandwidths [1–3]. First, the electronic support measurement (ESM) receiver is often non-cooperative with the radar transmitter and needs frequency wide open to cover most of the frequency range of hostile radar signals to complete effective interception. The ideal ESM receiver should be able to intercept the whole radar frequency range, namely about 18 GHz or 30 GHz. In addition, the digital ESM receiver, which is the main system for the current ESM, has many advantages over the analog one in signal processing flexibility and analysis precision. In conclusions, a good ESM receiver should combine

the wideband demand and the digital processing advantages. However, to the existing analog-to-digital converter (ADC) level of development, the sampling rate of commercially available off-the-shelf ADC is often less than 5 GHz, and it is difficult to directly sample the signals in radio frequency in such a wide frequency range about 18 GHz or 30 GHz. Therefore, how to use the existing ADC to sample the signal as wide as possible is a research hotspot for the ESM receiver.

In the past few decades, some methods on this topic have been presented. High speed interleaving/multiplexing data-acquisition system [4] is a typical technology which uses multiple low-speed ADCs to sample the signals alternately in time in order to improve the system's equivalent sampling rate. However, this method requires high time resolution and the channel timing correction. The design of hybrid filter banks for analog/digital conversion adopts a set of analog bandpass filters to reduce the bandwidth of each channel, and samples each channel with a low-speed ADC [5, 6]. Then, this kind of system needs a huge amount of equipment and has strict limitations in the performances of the filters. Analog-to-digital conversion via signal expansion is also a method to reduce the demands for ADC, and performs sampling in a transform domain, which is obtained by the signal projection on the spaces, such as frequency or wavelet space. For the signal reconstruction problem, this method requires a large number of low-speed ADCs to meet the accuracy requirements [7].

These technologies all use multiple low-speed ADCs to complete wideband signal acquisition, failing to solve the problems using single or dual low-speed ADCs to sample the whole interception wideband. Some new ways have been presented in the past few years. Compressed sensing (CS) theory [8–10] shows that if a signal is compressible or sparse in a certain transform domain, we can reconstruct the signal from the received signal with a high probability by introducing a signal independent observation matrix and an optimal solution algorithm. Typical CS receivers which could be used in ESM include the CS receiver using random demodulation [11] and the one with random filters for compressive sampling and reconstruction [12]. These two architectures both use one ADC. The distributed ultra-wideband amplifier receiver system is another kind of CS receiver which uses low-speed ADCs to achieve the sampling [13]. However, how to determine the sparse domains of the received signals in a non-cooperative case and quickly find the optimal solution still need to be studied.

Inspired by CS, Fudge proposed the Nyquist folding receiver (NYFR) [14]. The NYFR modulates the received analog signal in the front-end of the receiver, maps the Nyquist zone information to the modulation bandwidth of the signal, and then samples the modulated

signal. The Nyquist zone could be estimated from the bandwidth of the modulated signal. By changing the modulation type and the number of zones, we can use single or dual ADCs without frequency sweeping to cover the whole interception frequency in theory.

NYFR uses zero crossing rising voltage time to control the radio frequency sample clock and would be easily affected by noise. Moreover, the analog part and the digital part are not synchronized, and the initial phase of the received signal would be lost. This paper presents an improved structure marked as a synchronous NYFR (SNYFR) and shows an algorithm to the parameter estimation of classical linear frequency modulated (LFM) signal.

2. SNYFR

2.1. Structure for SNYFR

The structure of an SNYFR is shown in Fig. 1. To facilitate the follow-up derivation, we assume that the input analog signal has been preprocessed into I/Q signals. First, the input signal is filtered by a ultra wideband (UWB) filter (LPF$_1$), whose bandwidth is B_I, to remove the out-of-band noise to get the complex signal $x(t)$. Then, $x(t)$ is mixed by the UWB complex local oscillator signal (LOS) $p(t)$ to obtain the modulated signal $r(t) = x(t)p^*(t)$ where the mark $*$ stands for complex conjugation, and $r(t)$ is filtered by the second complex low-pass filter (LPF$_2$) $h(t)$ with the passband $[-f_s/2 \ f_s/2]$ to get the signal $s(t)$, where f_s is the sampling rate for digital signal processing. Finally, sample $s(t)$ by the rate f_s to obtain $x(n)$. The $p(t)$ is generated by the digital analog converter (DAC) and direct digital synthesizer (DDS),
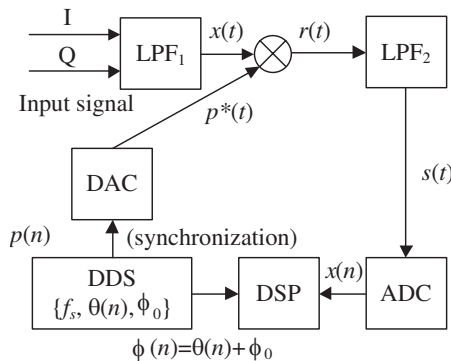
Figure 1. Block diagram of the SNYFR.

where the DDS is synthesized by the digital signal $p(n)$ which includes f_s, the phase $\theta(n)$ and the initial phase ϕ_0. The instantaneous phase $\phi(n) = \theta(n) + \phi_0$ corresponding to center frequency f_s of $p(n)$ is also sent to digital signal processor (DSP) for synchronization. B_I could be 18 GHz or 30 GHz. Note that this structure uses dual ADCs to cover the whole interception frequency range.

2.2. Output of SNYFR

We take the classical LFM signal as an example to determine the output of the SNYFR. Assume the signal after LPF_1 be

$$x(t) = Ae^{j[2\pi(f_0 t + K_0 t^2/2) + \phi_0]} + n_1(t) \tag{1}$$

where A, f_0, K_0 and ϕ_0 are the amplitude, frequency, chirp rate and initial phase, respectively. $n_1(t)$ is white Gaussian noise distributed in $[0 \ Kf_s)$. The noise power is N_0, and the power density is $N_0/(Kf_s)$. The signal to noise ratio (SNR) of $x(t)$ is A^2/N_0.

Define the kth Nyquist zone as $f \in [kf_s, (k+1)f_s)$, $k \in [0, K-1]$, where K is the number of zones. The NYFR adopts different bandwidths to represent different Nyquist zones, then the LOS could be

$$p(t) = \sum\nolimits_{k=0}^{K-1} e^{j\{2\pi f_s t/2 + k[2\pi f_s t + \theta(t) + \phi_{LOS}]\}} \tag{2}$$

where $\theta(t)$ and ϕ_{LOS} are the instantaneous phase and initial phase of the zone 1, respectively.

Then,

$$\begin{aligned}
r(t) &= x(t)p^*(t) \\
&= A\sum\nolimits_{k=0}^{K-1} e^{j[2\pi(f_0 t + K_0 t^2/2 - f_s t/2) + \phi_0 - k[2\pi f_s t + \theta(t) + \phi_{LOS}]]} \\
&\quad + n_1(t)\sum\nolimits_{k=0}^{K-1} e^{-j\{2\pi f_s t/2 + k[2\pi f_s t + \theta(t) + \phi_{LOS}]\}} \\
&= A\sum\nolimits_{k=0}^{K-1} e^{j\{2\pi(f_0 t + K_0 t^2/2 - f_s t/2) + \phi_0 - k[2\pi f_s t + \theta(t) + \phi_{LOS}]\}} + n_2(t) \quad (3)
\end{aligned}$$

where $n_2(t) = n_1(t) \sum_{k=0}^{K-1} e^{-j\{2\pi f_s t/2 + k[2\pi f_s t + \theta(t) + \phi_{LOS}]\}}$.

After filtered by LPF_2, we have

$$\begin{aligned}
s(t) &= r(t) \otimes h(t) \\
&= Ae^{j[2\pi(f_0 t + K_0 t^2/2 - f_s t/2) + \phi_0 - \beta_{f_0,K_0}(t)[2\pi f_s t + \theta(t) + \phi_{LOS}]]} \\
&\quad + n_3(t) \tag{4}
\end{aligned}$$

where $\beta_{f_0,K_0}(t) \approx \text{round}((f_0 + K_0 t - f_s/2)/f_s)$, $n_3(t) = n_2(t) \otimes h(t)$.

After sampling,

$$
\begin{aligned}
x(n) &= s(nT_s) \\
&= Ae^{j\left[2\pi\left(f_0 nT_s + K_0(nT_s)^2/2 - n/2\right) + \phi_0 - \beta_{f_0,K_0}(nT_s)[\theta(nT_s) + \phi_{LOS}]\right]} \\
&\quad + n_3(nT_s) \\
&= s_0(n) + n_3(nT_s)
\end{aligned}
\tag{5}
$$

where $s_0(n) = Ae^{j\phi_0}e^{\{j[2\pi(f_0 nT_s + K_0(nT_s)^2/2 - n/2) - \beta_{f_0,K_0}(nT_s)[\theta(nT_s) + \phi_{LOS}]]\}}$.

Equation (5) shows that $x(t)$ is turned into $x(n)$ through the SNYFR. As the digital signal $x(n)$ has a periodic frequency f_s, the digital frequency is just the remainder of the absolute frequency modulo f_s, losing the modulus information. However, $x(n)$ is modulated by additional LOS modulation $\beta_{f_0,K_0}(nT_s)[\theta(nT_s) + \phi_{LOS}]$, where $\beta_{f_0,K_0}(nT_s)$ is the modulus. In this case, the modulus and remainder have been both retained, hence we could recover the absolute frequency from the digital LOS modulation. For the amplitude and initial phase, $\theta(nT_s) + \phi_{LOS}$ is a prior, and if we estimate $\beta_{f_0,K_0}(nT_s)$ correctly, these parameters could also be estimated. In short, the SNYFR keeps the different parameters of the received signal $x(t)$ in different ways, so we do not lose the information of the signal.

The noise distribution is shown in Fig. 2. In $[-f_s/2, f_s/2]$, $n_3(t)$ and $n_3(nT_s)$ are both white Gaussian noise. The noise power is $\sum_{k=0}^{K-1} N_0/(Kf_s) = N_0$ and the power density is N_0/f_s. Then, the SNR of the output of the SNYFR is the same as the input of that, i.e., A^2/N_0, while, the output noise power density is much larger than the input one. Moreover, the relationship between B_I and K is

$$
B_I = Kf_s
\tag{6}
$$
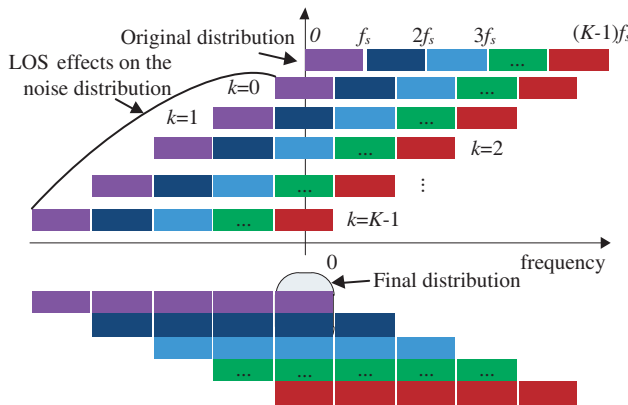
Figure 2. Noise distribution.

3. PARAMETER ESTIMATION OF THE RECEIVED SIGNAL

In ESM receiver, we mainly concern the estimation of frequency parameters, such as the initial frequency and chirp rate (or bandwidth), so we just estimate the two parameters. In order to facilitate the description of the principle, we assume that the received signal just contains a single LFM.

3.1. Maximum Likelihood Estimation

$x(n)$ could be expressed in matrix form,

$$\mathbf{x} = \mathbf{h}(\mathbf{d})A_0(\theta) + \mathbf{n}_3 \tag{7}$$

where $A_0(\theta) = A\exp(j\phi_0)$, $\mathbf{x} = [x(0), x(1), \ldots, x(N-1)]^T$, $\mathbf{d} = [\begin{array}{cc} f_0 & K_0 \end{array}]^T$, $\mathbf{h} = [h(0), h(1), \ldots, h(N-1)]^T$, $\theta = [\begin{array}{cc} A & \phi_0 \end{array}]^T$, $\mathbf{n}_3 = [n_3(0), n_3(1), \ldots, n_3(N-1)]^T$ and $h(n) = e^{j[2\pi(f_0 nT_s + K_0(nT_s)^2/2 - n/2) - \beta_{f_0,K_0}(nT_s)[\theta(nT_s) + \phi_{LOS}]]}$.

The probability density function of $x(n)$ is

$$p(\mathbf{x}; \mathbf{d}, \theta) = \frac{1}{\pi^N N_0^N} e^{-\frac{1}{N_0}[\mathbf{x} - \mathbf{h}(\mathbf{d})A_0(\theta)]^H[\mathbf{x} - \mathbf{h}(\mathbf{d})A_0(\theta)]} \tag{8}$$

The maximum likelihood (ML) estimation is

$$\left(\hat{\mathbf{d}}, \hat{\theta}\right) = \underset{\mathbf{d},\theta}{\arg\min} \left\{ [\mathbf{x} - \mathbf{h}(\mathbf{d})A_0(\theta)]^H [\mathbf{x} - \mathbf{h}(\mathbf{d})A_0(\theta)] \right\} \tag{9}$$

Then,

$$\hat{\mathbf{d}} = \underset{\mathbf{d}}{\arg\max} \left\{ \mathbf{x}^H \left\{ \mathbf{h}(\mathbf{d}) \left[\mathbf{h}^H(\mathbf{d})\mathbf{h}(\mathbf{d})\right]^{-1} \mathbf{h}^H(\mathbf{d}) \right\} \mathbf{x} \right\}$$

$$= \underset{\mathbf{d}}{\arg\max} \frac{1}{N} \left\{ \left(\mathbf{h}^H(\mathbf{d})\mathbf{x}\right)^H \mathbf{h}^H(\mathbf{d})\mathbf{x} \right\} \tag{10}$$

$$A_0\left(\hat{\theta}\right) = \frac{1}{N}\mathbf{h}^H\left(\hat{\mathbf{d}}\right)\mathbf{x} \tag{11}$$

We could estimate the parameters of $x(t)$ from (10) and (11).

3.2. Fast Parameter Estimation Algorithm

The ML algorithm for the estimation of the initial frequency and chirp rate needs a two dimension search, where the frequency search range should be from 0 to 18 GHz or 30 GHz. Taking the step size 10 KHz as an example, we need about $(30\,\mathrm{G}/10\,\mathrm{K}) \times (30\,\mathrm{G}/10\,\mathrm{K}) = 9 \times 10^{12}$ grid

search to determine the estimation. This computational complexity is heavy. We present the following fast estimation algorithm.

First, we consider the condition that the signal is just in one Nyquist zone, i.e., $f_0 + K_0 t \in [k f_s \ (k+1) f_s)$, then $\beta_{f_0, K_0}(n T_s) \approx k_{f_0}$, and

$$
\begin{aligned}
x(n) &= A e^{j\left[2\pi\left(f_0 n T_s + K_0 (n T_s)^2/2 - n/2\right) + \phi_0 - k_{f_0}[\theta(n T_s) + \phi_{LOS}]\right]} \\
&\quad + n_3(n T_s) \\
&= A e^{j\left[2\pi\left(f_0 n T_s + K_0 (n T_s)^2/2 - n/2\right) + \phi_0\right]} e^{j\left[-k_{f_0}[\theta(n T_s) + \phi_{LOS}]\right]} \\
&\quad + n_3(n T_s) \\
&= A x_{LFM}(n) x_{LOS}(n) + n_3(n T_s)
\end{aligned}
\tag{12}
$$

Let $y_k(n) = x(n) x_{LOS}^{(k)}(n)$, where $x_{LOS}^{(k)}(n) = e^{j[k[\theta(n T_s) + \phi_{LOS}]]}$, then

$$
\begin{aligned}
y_k(n) &= \left[A x_{LFM}(n) x_{LOS}(n) + n_3(n T_s)\right] x_{LOS}^{(k)}(n) \\
&= A x_{LFM}(n) x_{LOS}(n) x_{LOS}^{(k)}(n) + n_3(n T_s) x_{LOS}^{(k)}(n) \\
&= A x_{LFM}(n) x_{LOS}^{(k-k_{f_0})}(n) + n_3(n T_s) x_{LOS}^{(k)}(n)
\end{aligned}
\tag{13}
$$

When $k \neq k_{f_0}$, $x_{LFM}(n)$ has a convolution with $x_{LOS}^{(k-k_{f_0})}(n)$ in frequency, extending the range of the spectrum of the pure signal. Since the total energy is constant, compared with $k = k_{f_0}$, the energy for each unit of frequency for the pure signal would drop, and the maximum energy of the spectrum will be correspondingly reduced. Moreover, $n_3(n T_s)$ would also have a convolution with $x_{LOS}^{(k)}(n)$ in frequency, and the distribution of noise would be changed. If the SNR for $y_k(n)$ is high enough that the spectrum peak of $A x_{LFM}(n) x_{LOS}^{(k-k_{f_0})}(n)$ is higher than the one of $n_3(n T_s) x_{LOS}^{(k)}(n)$, the maximum value of the spectrum of $y_{k_{f_0}}(n)$ would be the maximum in all k. Further, a greater spectrum peak would be got for those $x_{LOS}^{(k)}(n)$ with smaller wideband, then the distribution of the noise for different k would be different.

In summary, we can do Fourier transform for all $y_k(n)$, and determine k, where the maximum value of the Fourier transform is the largest, as the estimation of k_{f_0}. The probability of correct decision (PCD) for small k_{f_0} would be less than the one for large k_{f_0}.

There are some advices for choosing the LOS. From the previous paragraph, we know that the PCD would be related with the bandwidth of the LOS for different k_{f_0}. If we want to have the same PCD for different k_{f_0}, the bandwidths for different k_{f_0} should be the same. Then, the LOS could have the same bandwidth for different k_{f_0} and the Nyquist zone information should be contained

in other parameter rather than bandwidth. We could adopt phase shift-keying (PSK) signal which has different codes in different zones to modulate the received signal, and demodulate the signal in digital part to estimate the zones. However, the spectrum of PSK has a larger variance, so is the variance of $n_3(nT_s)x_{LOS}^{(k)}(n)$, making the difference between the maximum of spectrum of pure signal and the noise smaller. Then, the ideal LOS needs a smaller variance in spectrum. Consequently, the zone-dependent white noise with fixed bandwidth for different zones is one kind of ideal LOS.

Second, when LFM belongs to two zones, namely the k_{f_0}th and $k_{f_0} + 1$th zones, and $n = N_0$ is the turning point from the k_{f_0}th to $k_{f_0} + 1$th zone, then

$$
\begin{aligned}
x(n) &= Ae^{j\left[2\pi(f_0 nT_s + K_0(nT_s)^2/2 - n/2) + \phi_0 - k_{f_0}[\theta(nT_s) + \phi_{LOS}]\right]}\mu(1, N_0) \\
&+ Ae^{j\left[2\pi(f_0 nT_s + K_0(nT_s)^2/2 - n/2) + \phi_0 - (k_{f_0}+1)[\theta(nT_s) + \phi_{LOS}]\right]}\mu(N_0 + 1, N) \\
&+ n_3(nT_s) \\
&= Ae^{j\left[2\pi(f_0 nT_s + K_0(nT_s)^2/2 - n/2) + \phi_0 - k_{f_0}[\theta(nT_s) + \phi_{LOS}]\right]}\kappa(N_0) + n_3(nT_s) \\
&= Ax_{LFM}(n)x_{LOS}(n)\kappa(N_0) + n_3(nT_s) \tag{14}
\end{aligned}
$$

where $\mu(a, b) = \begin{cases} 1, & n \in [a, b] \\ 0, & \text{otherwise} \end{cases}$ and $\kappa(N_0) = \mu(1, N_0) + e^{-j[\theta(nT_s) + \phi_{LOS}]}\mu(N_0 + 1, N)$.

Then,

$$
\begin{aligned}
y_k(n, N_0) &= [Ax_{LFM}(n)x_{LOS}(n) + n_3(nT_s)]x_{LOS}^{(k)}(n)\kappa^*(N_0) \\
&= Ax_{LFM}(n)x_{LOS}(n)\kappa(N_0)x_{LOS}^{(k)}(n)\kappa^*(N_0) \\
&\quad + n_3(nT_s)x_{LOS}^{(k)}(n)\kappa^*(N_0) \tag{15}
\end{aligned}
$$

Similar to the condition that the LFM signal is just in one Nyquist zone, we can compute the Fourier transform of $y_k(n, N_0)$ under different k and N_0, and treat the k and N_0 whose maximum spectrum is the largest as the estimates of N_0 and k_{f_0}.

Finally, when the LFM signal belongs to M different zones, assume $N_0, N_1, \ldots, N_{M-1}$ are the turning points, then

$$
x(n) = Ax_{LFM}(n)x_{LOS}(n)\kappa(N_0, N_1, \ldots, N_{M-1}) + n_3(nT_s) \tag{16}
$$

where $\kappa(N_0) = \mu(1, N_0) + e^{-j[\theta(nT_s) + \phi_{LOS}]}\mu(N_0 + 1, N_1) + e^{-j2[\theta(nT_s) + \phi_{LOS}]} \times \mu(N_1 + 1, N_2) + \ldots + e^{-j(M-1)[\theta(nT_s) + \phi_{LOS}]}\mu(N_{M-1} + 1, N)$.

Since the instantaneous frequency of the LFM signal is proportional to time, then we have

$$
\Delta N = N_2 - N_1 = N_3 - N_2 = \ldots = N_{M-1} - N_{M-2} \tag{17}
$$

That is to say, $[N_1, N_2, \ldots, N_{M-1}]$ is an arithmetic sequence, so $\kappa(N_0, N_1, \ldots, N_{M-1})$ in (16) could be rewritten as $\kappa(N_0, N_1, N_1 + \Delta N, N_1 + 2\Delta N, \ldots, N_1 + (M-2)\Delta N)$. Then there are just three variables $\{N_0, N_1, \Delta N\}$ in κ, and we can reduce the computational complexity during the grid search.

From the above analysis, when the parameters $\{N_0, N_1, \Delta N, k\}$ of $x_{LOS}(n)\kappa(N_0, N_1, \ldots, N_{M-1})$ are matched with the received signal, we could get the under-sampling signal in (16). For the LFM case, the signal is still the broadband signal, and the aggregation in frequency, which is equivalent to the processing gain in frequency, is poor. As the single tone has the best aggregation in frequency, if we could turn the LFM signal into a single tone, the processing in frequency would be much easier. Then the LFM signal could be delayed and have a conjugated multiplication with the original signal [15], and the signal is converted to a single tone to improve the aggregation in frequency to get a higher gain to improve noise immunity.

If the Nyquist zones are estimated, we could do the parameter estimation with the fast dechirp algorithm [15] which transforms the estimation of initial frequency and chirp rate (or bandwidth) of the LFM signal into the estimation of two single tones. Note that the estimation of the single frequency of chirp rate $\hat{K}_0$ would be located in Nyquist zone zero, there is no frequency ambiguity problem. However, we should add Nyquist zone k_{f_0} to the estimation of the initial frequency.

4. SIMULATION RESULTS

Simulations have been done to verify the performances of the proposed method. We define PCD and root mean square error (RMSE) to evaluate the performances of the Nyquist zone detection and parameter estimation of the LFM signal:

$$\text{PCD} = \sum_{q=0}^{Q} (\hat{x}_q = x)/Q \tag{18}$$

The ML is equivalent to

$$\text{RMSE} = \sqrt{\sum_{q=0}^{Q-1} (\hat{x}_q - x)^2/Q}/f_s \tag{19}$$

where x is the true value, $\hat{x}_q$ is the estimate of the qth experiment, the " $=$ " of $\hat{x}_q = x$ in (18) is a logic symbol, where the value of $\hat{x}_q = x$ is 1 when $\hat{x}_q$ is equal to x, otherwise 0. Q is the number of experiment.

$\theta(t)$ of LOS is a sinusoidal FM signal with modulation bandwidth 40 MHz, modulation cycle 0.2 μs. The sampling rate $f_s = 1$ GHz.

4.1. The Outputs of SNYFR, Under-sampling and Nyquist Sampling

The initial frequency and bandwidth of the LFM signal are 6.3 GHz and 1.5 GHz, respectively. The pulse width is 1 μs. The sampling rate for under-sampling and Nyquist sampling are 1 GHz and 18 GHz, respectively. In order to facilitate comparison, we do 500 MHz digital down-conversion to the signal before under-sapling. Fig. 3 shows the instantaneous frequencies for each sampling. It's found that, the under-sampling contains the remainder of the absolute frequency modulo sampling rate, losing the modulus information. While, the SNYFR keeps the modulus which could be used to recover the signal.

4.2. Nyquist Zone Detection Performance

In Section 3, we discussed the Nyquist zone detection algorithms where the LFM signal lies in one zone and multi-zones, respectively. In simulations, we simulate one zone condition with the 6th zone where the initial frequency is 6.3 GHz and the bandwidth are 0.2 MHz, 0.5 MHz and 0.7 MHz, and two zones condition with 6th and 7th zones where the initial frequency is 6.3 GHz and the bandwidth are 0.8 GHz, 1 GHz and 1.5 GHz. The pulse widths are 0.5 μs and 1 μs. Fig. 4(a) shows the one zone condition. When the SNR is greater than −4 dB, the PCD is greater than 90%. Fig. 4(b) shows the two zones condition and the PCD is greater than 90% when the SNR is greater than −3 dB. Compared with the one zone case, the detection of the multi-zones needs to estimate additional parameters, and there are some performance loss. Moreover, the PCD corresponding to long
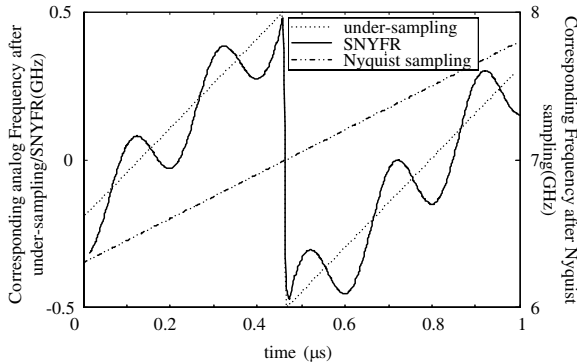
Figure 3. Output instantaneous frequencies of SNYFR, undersampling and Nyquist sampling.

(a) PCD VS SNR where LFM lies in one Nyquist zone.

(b) PCD VS SNR where LFM lies in two Nyquist zones.
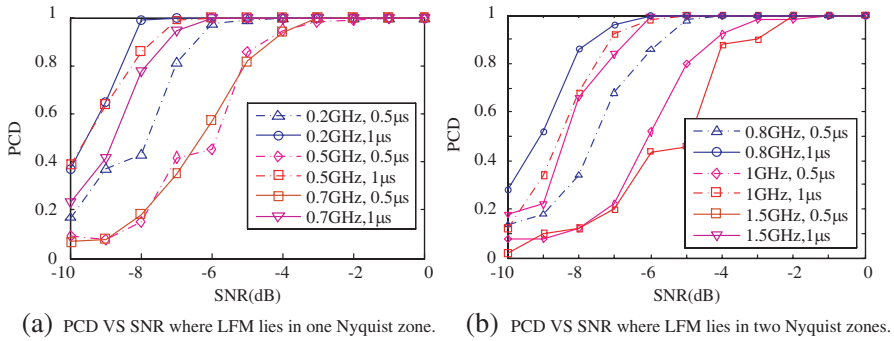
Figure 4. PCD VS SNR.
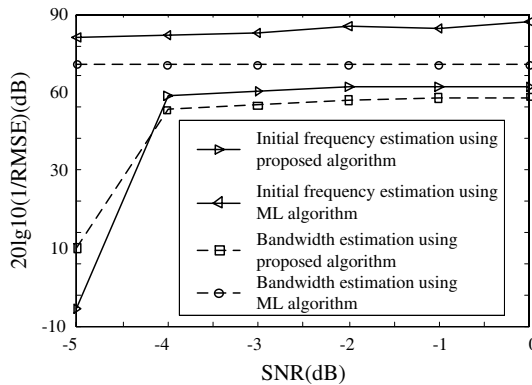
Figure 5. Performance comparison between the proposed algorithm and the ML.

pulse width is greater than those of short pulse widths due to the time accumulation effect. For the same pulse width, the PCD corresponding to greater bandwidth would be smaller than those corresponding to smaller bandwidths due to the expanding effect of wideband signal in frequency.

4.3. Parameter Estimation of the LFM Signal

After zone detection, we estimate the parameters using the ML estimation and fast algorithms, respectively. The initial frequency and bandwidth are $6.373111\,\text{GHz}$ and $0.5872111\,\text{GHz}$, respectively. The pulse width is $0.5\,\mu\text{s}$. The results are shown in Fig. 5. When the SNR is greater than $-4\,\text{dB}$, the performance is close to the ML one.

4.4. Computational Complexity of the Proposed Algorithm for SNYFR

We take the condition where LFM lies in two Nyquist zones as an example to show the computational complexity of the proposed algorithm. Assume that the interception wideband and sampling rate are $30\,\text{GHz}$ and $1\,\text{GHz}$, respectively, and the number of samples is $N = 1024$. Then, we have $K = 30$. Since $k_{f_0} \in [0, K-1]$ and for SNYFR, we just need to search $NK = 1024 \times 30 = 30720$ grids to find the maximum value to estimate the k_{f_0} and N_0 to determine the Nyquist zone information. For the estimation of parameters of LFM, we just need two fast Fourier transforms [15], which could be ignored compared with the grid search. So, the computational complexity is far less than the one of ML.

5. CONCLUSION

We proposed the SNYFR which could sample the wideband signal located in multi-Nyquist zones using two ADCs. Taking the LFM signal as an example, we showed that the output SNR was equal to the input one, while, the noise power density was much higher than the input one. The algorithm for the estimation of the LFM signal located in multi-zones was also discussed, and the performance was stable when SNR was greater than $-3\,\text{dB}$. Note that we proposed a prototype for SNYFR using different bandwidths to represent different zones. Using other modulations to represent the zones and exploiting their corresponding parameter estimation algorithms are in the next step of the research content. Moreover, the processing of multiple signals and detection of Nyquist zones in the well developed signal detection framework will be detailed further.

REFERENCES

1. Jiang, T., S. Qiao, Z.-G. Shi, L. Peng, J. Huangfu, W.-Z. Cui, W. Ma, and L.-X. Ran, "Simulation and experimental evaluation of the radar signal performance of chaotic signals generated from a microwave colpitts oscillator," *Progress In Electromagnetics Research*, Vol. 90, 15–30, 2009.

2. Lazaro, A., D. Girbau, and R. Villarino, "Wavelet-based breast tumor localization technique using a UWB radar," *Progress In Electromagnetics Research*, Vol. 98, 75–95, 2009.

3. Chen, D. and C.-H. Cheng, "A novel compact ultra-wideband (UWB) wide slot antenna with via holes," *Progress In Electromagnetics Research*, Vol. 94, 343–349, 2009.

4. Zhang, J., J. Wu, W. Liu, C. Qiao, and L. Wang, "Clock study of high speed interleaving/multiplexing data-acquisition system," *Journal of University of Science and Technology of China*, Vol. 36, No. 3, 281–284, 2006.

5. Velazquez, S. R., T. Q. Nguyen, and S. R. Broadstone, "Design of hybrid filter banks for analog/digital conversion," *IEEE Trans. Signal Processing*, Vol. 46, No. 4, 956–967, 1998.

6. Namgoong, W., "A channelized digital ultrawideband receiver," *IEEE Trans. Wireless Communications*, Vol. 2, No. 3, 502–510, 2003.

7. Hoyos, S., B. M. Sadler, and G. R. Arce, "Ultra-wideband analog-to-digital conversion via signal expansion," *IEEE Trans. Vehicular Technology*, Vol. 54, No. 5, 1609–1622, 2005.

8. Donoho, D. L., "Compressed sensing," *IEEE Trans. Information Theory*, Vol. 52, No. 4, 1289–1306, 2006.

9. Chi, Y. J., L. L. Scharf, A. Pezeshki, and A. R. Calderbank, "Sensitivity to basis mismatch in compressed sensing," *IEEE Trans. Signal Processing*, Vol. 59, No. 5, 2182–2195, 2011.

10. Migliore, M. D., "A compressed sensing approach for array diagnosis from a small set of near-field measurements," *IEEE Trans. Antennas and Propagation*, Vol. 59, No. 6, 2127–2133, 2011.

11. Laska, J. N., S. Kirolos, M. F. Duarte, T. S. Ragheb, R. G. Baraniuk, and Y. Massoud, "Theory and implementation of an analog-to-information converter using random demodulation," *IEEE International Symposium on Circuits and Systems*, 1959–1962, 2007.

12. Tropp, J. A., M. B. Wakin, M. F. Duarte, D. Baron, and R. G. Baraniuk, "Random filters for compressive sampling and reconstruction," *IEEE International Conference on Acoustics, Speech and Signal Processing*, 872–875, 2006.

13. Yang, D., H. Li, G. D. Peterson, and A. Fathy, "Compressed sensing based UWB receiver: hardware compressing and FPGA reconstruction," *43rd Annual Conference on Information Sciences and Systems*, 198–201, 2009.

14. Fudge, G. L., R. E. Bland, M. A. Chivers, S. Ravindran, J. Haupt, and P. E. Pace, "A Nyquist folding analog-to-information receiver," *42nd Asilomar Conference on Signals, Systems and Computers*, 541–545, 2008.

15. Liu, Y., "Fast dechirp algorithm," *Journal of Data Acquisition and Processing*, Vol. 14, No. 2, 175–178, 1999.